

## Supplemental Material for

### **Post-transcriptional control of executioner caspases by RNA-binding proteins**

Deni Subasic, Thomas Stoeger, Seline Eisenring, Ana M. Matia-González, Jochen Imig, Xue Zheng, Lei Xiong, Pascal Gisler, Ralf Eberhard, René Holtackers, André P. Gerber, Lucas Pelkmans and Michael O. Hengartner

Corresponding author e-mail: [michael.hengartner@imls.uzh.ch](mailto:michael.hengartner@imls.uzh.ch)

**This PDF file includes:**

Supplemental Figures S1 to S10

Supplemental Tables S1 to S4

References

## Supplemental Figures S1 to S10

### Supplemental Figure S1. Apoptotic pathways in *C. elegans*, *D. melanogaster* and mammals are evolutionarily conserved

Functional homologs involved in apoptosis regulation between these species are shown in the same colour. Caspase activation is the last step of the canonical apoptotic cascade. While mammals and *Drosophila* have separate initiator and executor caspases, in *C. elegans*, CED-3 serves both functions. The inhibitors of apoptosis (IAPs) proteins can directly inhibit activated caspases in *Drosophila* and mammals, and their function is subject to negative regulation by Hid/Reaper/Grim/Sickle in *Drosophila* and Smac/Diablo in mammals.

### Supplemental Figure S2. CED-3::GFP localization in the germline is mostly nuclear

(A, B) DIC and GFP photomicrographs of early meiotic zone (a) and oocyte zone (b) of an adult hermaphrodite expressing CED-3::GFP ( $P_{ced-3}::ced-3::gfp::ced-3(3'UTR)$ ). Scale bar: 10  $\mu$ m.

### Supplemental Figure S3. *gld-1(RNAi)* affects the expression of the wild-type *ced-3* 3'UTR reporter, but not of the reporter with two GBM mutations

Fluorescence photomicrographs of adult *C. elegans* gonads expressing *ced-3* 3'UTR reporter ( $P_{pie-1}::gfp::h2b::ced-3$  3'UTR) and *ced-3* GBM 1,2 mt 3'UTR reporter treated with *Empty Vector Control(RNAi)* and *gld-1(RNAi)*. Gonads are outlined with a dashed line and arrowheads indicate the position of the distal tip cell. Average MFIs measured in the four germline zones and fertilized embryos from  $\geq 10$  animals are plotted. Error bars represent SEM ( $n \geq 10$ ) and asterisks indicates significant p-values ( $*p < 0.0001$ ). Scale bar: 10  $\mu$ m. NA, not applicable (*gld-1(RNAi)*-treated animals fail to produce oocytes).

### Supplemental Figure S4. Introducing *cgh-1(ok492)*, *puf-8(ok302)* and *gld-1(op236)* mutants in CED-3::GFP translational reporter recapitulates the RNAi-induced increase in CED-3 abundance increase in different regions of the germline

(A, B) DIC and GFP images of adult gonads expressing CED-3::GFP reporter with and without *cgh-1(ok492)* or *puf-8(ok302)* mutation in the background. Dashed lines outline the gonads and arrowheads indicate the position of the distal tip cell. Different zones selected for quantification (as in (D)) are separated with straight dashed white line. Average MFI

measured in four areas of the germline is represented on the chart. Error bars indicate SEM ( $n \geq 15$  for a) and  $n \geq 8$  for b)) and significant p-values are indicated with an asterisk (\* $p < 0.05$ , \*\* $p < 0.0001$ ). Scale bar: 10  $\mu\text{m}$ .

(C) DIC and GFP images of dissected adult gonads expressing CED-3::GFP reporter with and without *gld-1(op236ts)* mutation in the background. Animals were raised at 25°C to induce expression of the *gld-1(op236)* phenotype (Schumacher et al. 2005). Different zones selected for quantification (as in (D)) are separated with straight dashed white line and arrowheads indicate the position of the distal tip cell. Error bars indicate SEM ( $n \geq 15$ ) and significant p-values are indicated with an asterisk (\* $p < 0.05$ , \*\* $p < 0.0001$ ). Scale bar: 10  $\mu\text{m}$ .

### **Supplemental Figure S5. *ced-3* 3'UTR reporters in which predicted PUF-8 (PBM) and MEX-3 binding motifs (MBM) were mutated do not show any change in GFP expression pattern**

(A) Sequence alignment of *ced-3* 3'UTRs from five *Caenorhabditis* species: *C. elegans*, *C. remanei*, *C. briggsae*, *C. brenneri* and *C. japonica*. Level of sequence conservation is indicated in the colour heat map on the top left. The two GLD-1 binding motifs (GBMs) identified in HITS-CLIP and PAR-CLIP experiment (Brümmer et al. 2013; Jungkamp et al. 2011), the four predicted PUF-8 binding motifs (PBMs) (Opperman et al. 2005) and the two predicted MEX-3 binding motifs (MBMs) (Pagano et al. 2009) are marked with black, green and red boxes, respectively. The seed sequences of three miRNAs miR-785, miR-86 and miR-792 predicted to base pair with *ced-3* 3'UTR and positioned in the vicinity of GBM1 are marked with a blue, orange and pink line, respectively.

(B) Mutations used to generate *ced-3* GBM 1,2 mt, *ced-3* PBM 1,2,3,4 mt and *ced-3* MBM 1,2 mt 3'UTR reporters.

(C, D) Fluorescence photomicrographs of adult *C. elegans* gonads expressing wild-type *ced-3* 3'UTR reporter (*Ppie-1::gfp::h2b::ced-3* 3'UTR) and *ced-3* MBM 1,2 mt 3'UTR reporter (b) or *ced-3* PBM 1,2,3,4 mt 3'UTR reporter (c). Gonads are outlined with a dashed line and arrowheads indicate the position of the distal tip cell. Average MFIs measured in the four germline zones and fertilized embryos from  $\geq 10$  animals are plotted. Error bars represent SEM ( $n \geq 10$ ). Scale bar: 10  $\mu\text{m}$ .

### **Supplemental Figure S6. Mutating the seed sequence of miR-785, miR-86 and miR-792 does not affect *ced-3* expression levels**

Fluorescence photomicrographs of adult *C. elegans* gonads expressing wild-type *ced-3* (*Ppie-1::gfp::h2b::ced-3* 3'UTR), *ced-3* miR-785/86/792 mt, *ced-3* GBM 1 mt, and *ced-3* GBM 1 mt + miR-785/86/792 mt 3'UTR reporters. Gonads are outlined with a dashed line and arrowheads indicate the position of the distal tip cell. Average MFIs measured in the four germline zones and fertilized embryos from  $\geq 15$  animals are plotted. Error bars represent SEM ( $n \geq 15$ ) and asterisks indicates significant p-values ( $*p < 0.001$ ). Scale bar: 10  $\mu\text{m}$ .

### **Supplemental Figure S7. Executioner caspase 3'UTRs are unusually long**

Executioner caspase 3'UTR lengths in *C. elegans* (A), *D. rerio* (B), *X. tropicalis* (C), *O. cuniculus* (D) and *H. Sapiens* (E) are marked on histograms indicating the frequency of 3'UTRs of a given length within the respective species. Percentiles for the executioner caspase 3'UTR length within a species are indicated in the brackets. (F) Schematic representation of experimental and predicted binding motifs of *H. sapiens* caspase-3 3'UTR (1,574 bp, NM\_004346, NM\_032991). Experimental data has been extracted from AURA database (Dassi et al. 2014) (<http://aura.science.unitn.it/>) which compiles published CLIP experiments. Red, blue and purple boxes indicate the position within the 3'UTR where FMR1, FXR2 and FXR1 bind, respectively (Ascano et al. 2012). Patterned boxes indicate the position of CLIP coverage PUM1/2 (Hafner et al. 2010; Khorshid et al. 2011). Black and green boxes indicate the position of the predicted binding motifs within caspase-3 3'UTR, based on experimentally verified RNA binding sites for QKI (Galarneau and Richard 2005) and PUM1/2 (Wang et al. 2002) respectively; motif conservation across species was analysed by BLAT (Kent 2002) alignment (UCSC Browser (Kent et al. 2002)). Dash line represents PABPC1, PUM1 and PUM2 binding of caspase-3 observed by RIP-chips (Mukherjee et al. 2009; Galgano et al. 2008; Morris et al. 2008).

### **Supplemental Figure S8. Correlation between two replicate wells in a siRNA based screen for human caspase-3 3'UTR regulation**

(A) Comparison of the number of cells per well between two technical replicate wells on the same multi-well plate. Candidate siRNA indicate individual siRNAs against RNA Binding Proteins. No siRNA indicates mock transfections with Opti-MEM. siRNA against PLK1, a mitotic cycle regulator essential for viability, was used as a positive control for reduced cell

number. siRNAs resulting in a lower number of cells than the number of seeded cells were considered as cell killers and excluded from further analysis.

(B) Reporter upregulation was defined as the fraction of cells with a given intensity measurement above a given threshold. Black box indicates the combination of intensity measurement (median GFP intensity in nucleus) and threshold value shown in Figure 4. Heatmaps shows the Spearman correlation of the fraction of cells with GFP::caspase-3 3'UTR reporter activity across all wells of two technical replicates for several alternate definitions of reporter activity. Threshold indicates increasing grayscale values (measured in Arbitrary Units).

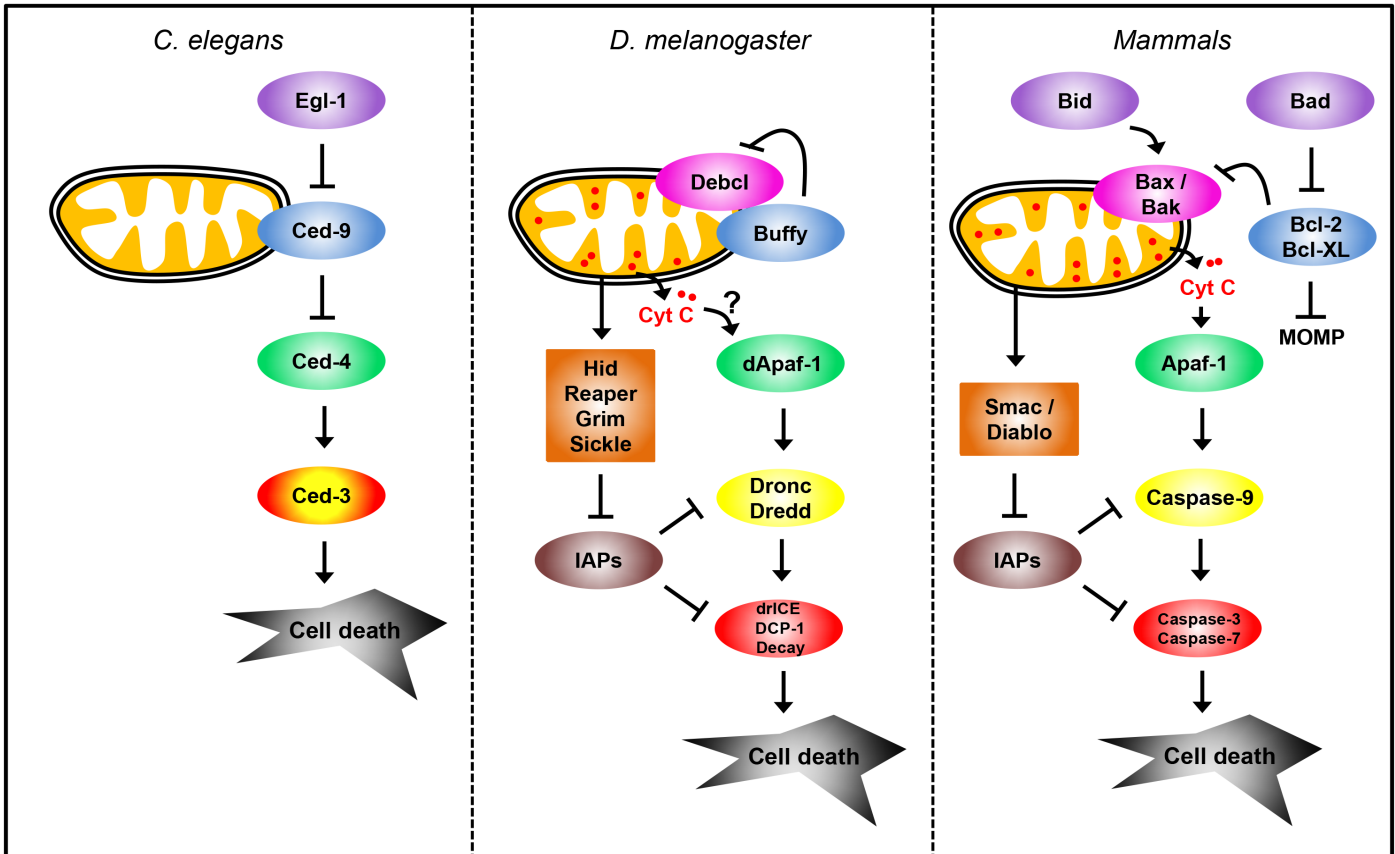
### **Supplemental Figure S9. Significance of elevated level of GFP::caspase-3 3'UTR reporter following knock-down of RBP candidates in the image-based screen**

Upregulation of GFP::caspase-3 3'UTR reporter activity was tested by  $p < 0.05$  (Fisher's exact test) compared to negative control wells (no siRNA or SilencerSelect scrambled siRNA). As there were multiple wells of negative controls, the heatmaps of this supplemental figure shows the fraction of all pairwise comparisons, where  $p < 0.05$  is met. In addition the boxplot shows different threshold levels and single-cell intensity readouts to illustrate that findings hold independently of the specific parameter values. Thresholds are given in grayscale values (measured in Arbitrary Units).


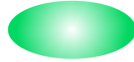
### **Supplemental Figure S10. Caspase-3 is regulated by RBPs largely at the post-transcriptional level**

(A) Changes in CASP3 protein levels upon siRNA-mediated knock-down of candidate RBPs identified in the screen. Total CASP3 protein abundance was measured by western blot. Error bars represent SEM (N=3 biological replicates). \*  $p \leq 0.05$  (paired t-test).

(B) Changes in CASP3 protein levels upon siRNA-mediated knock-down of candidate RBPs identified in the screen measured by bDNA single molecule fluorescence *in situ* hybridization. Error bars represent SEM (N=3 biological replicates). \*  $p \leq 0.05$  (paired t-test).

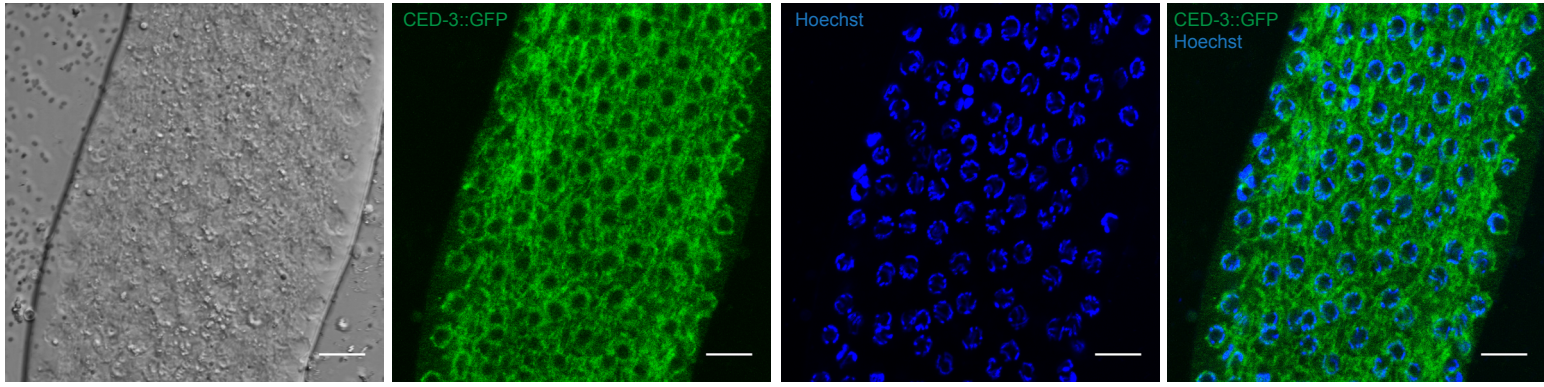


 Pro-apoptotic BH3 only Bcl-2  
 Pro-apoptotic multidomain Bcl-2

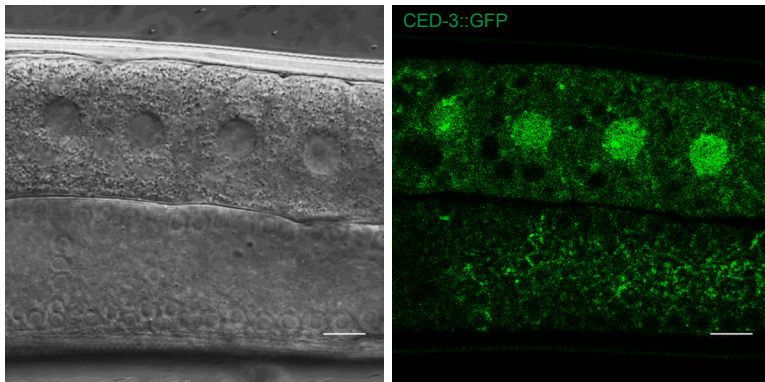
 Anti-apoptotic multidomain Bcl-2  
 Caspase activator

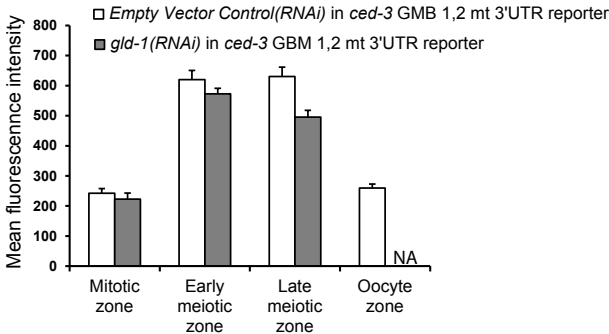
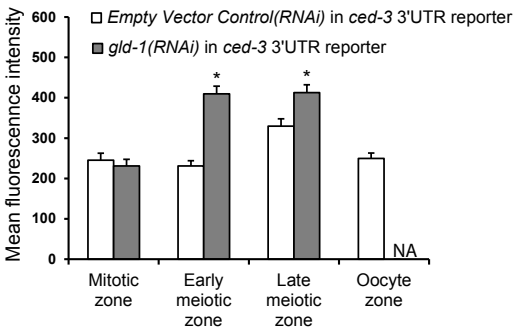
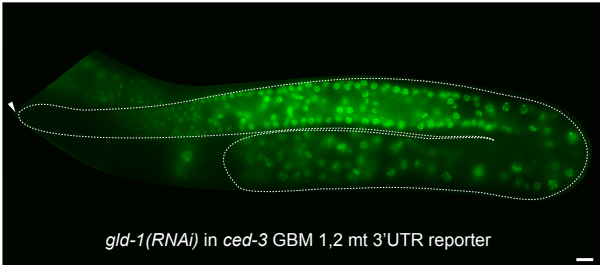
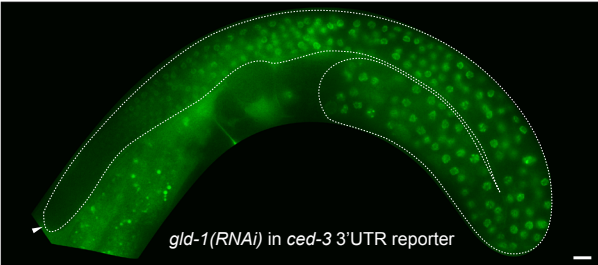
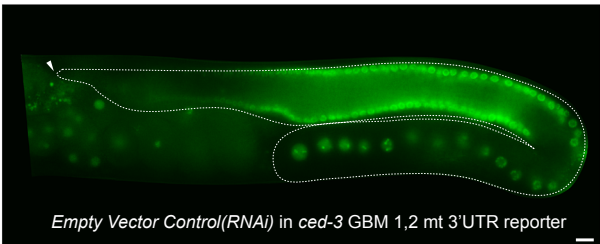
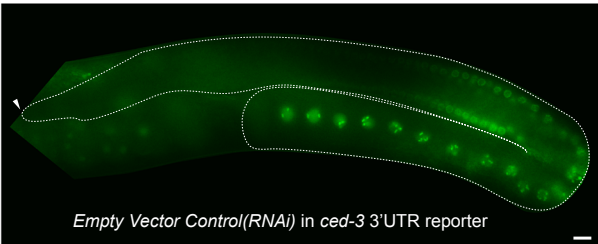
 Initiator caspase  
 Executioner caspase

**A**



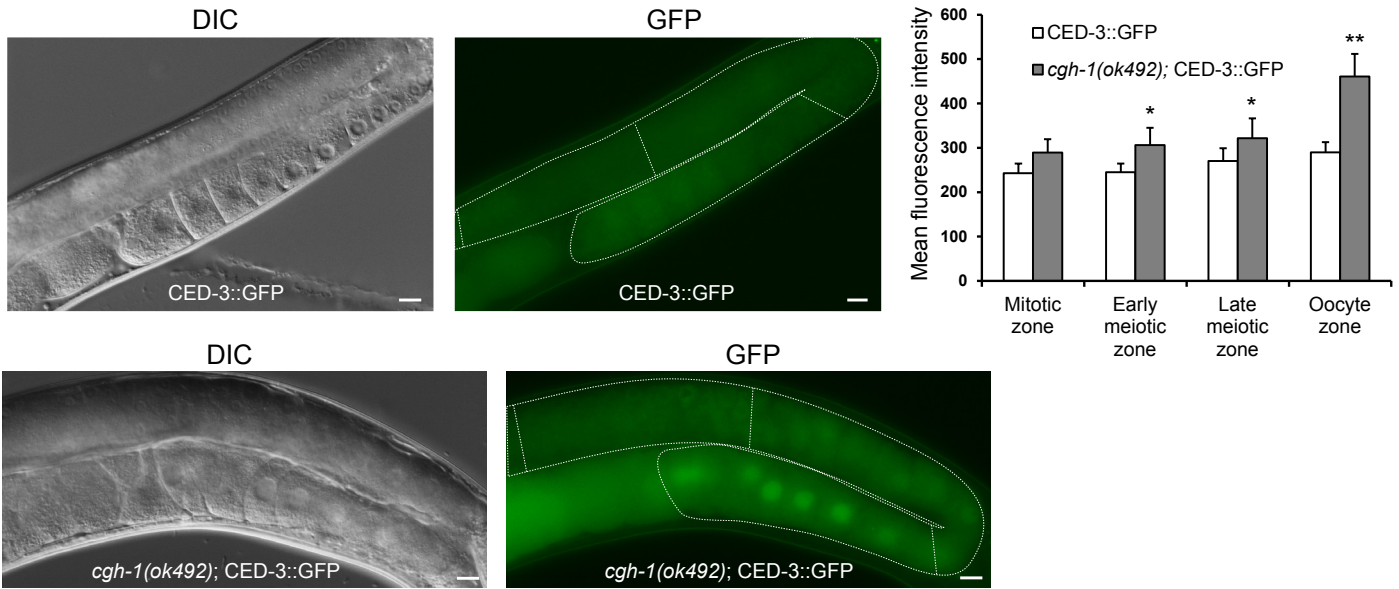
**B**



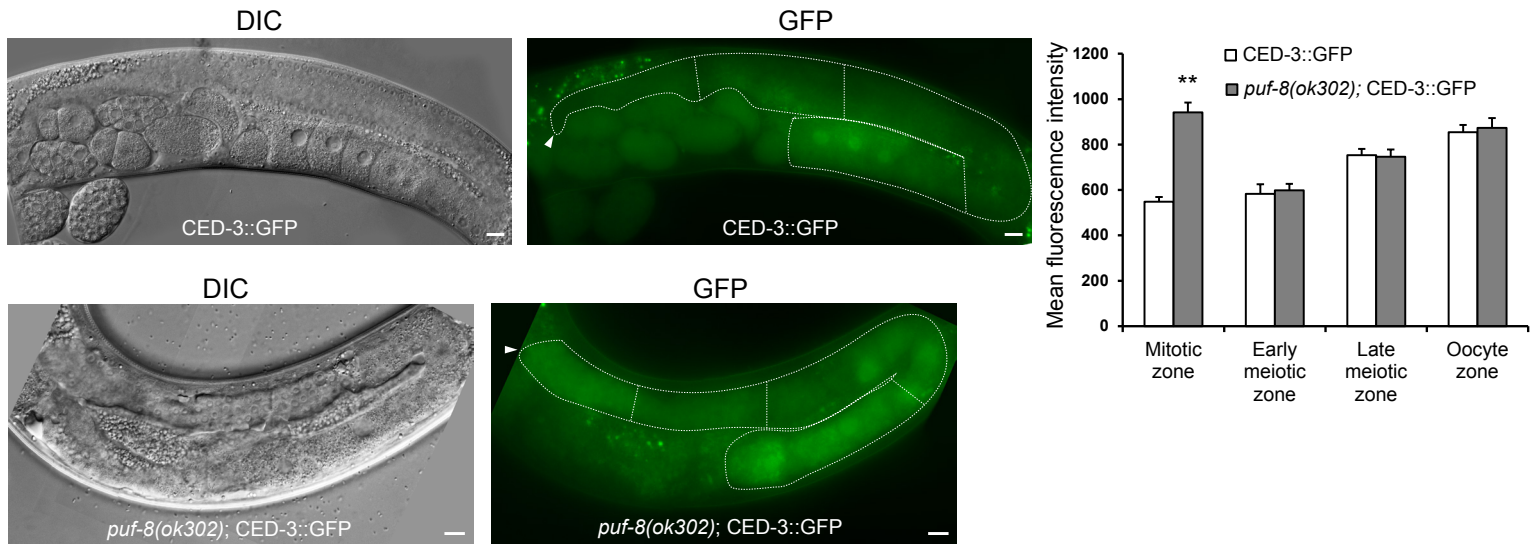




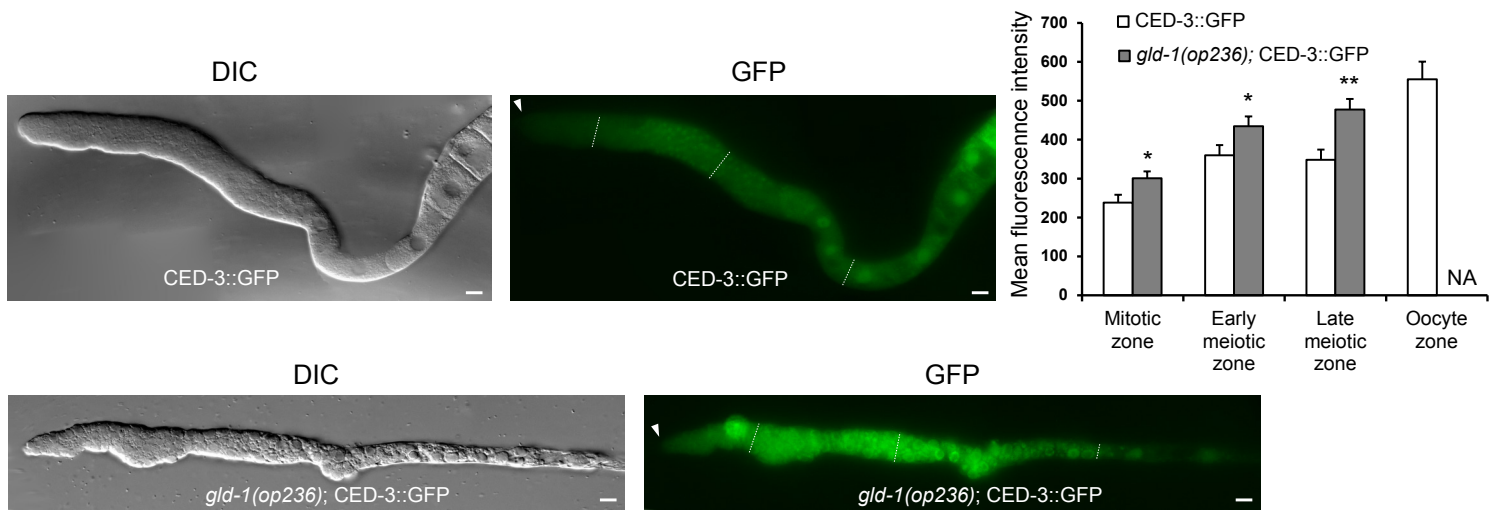
**A**



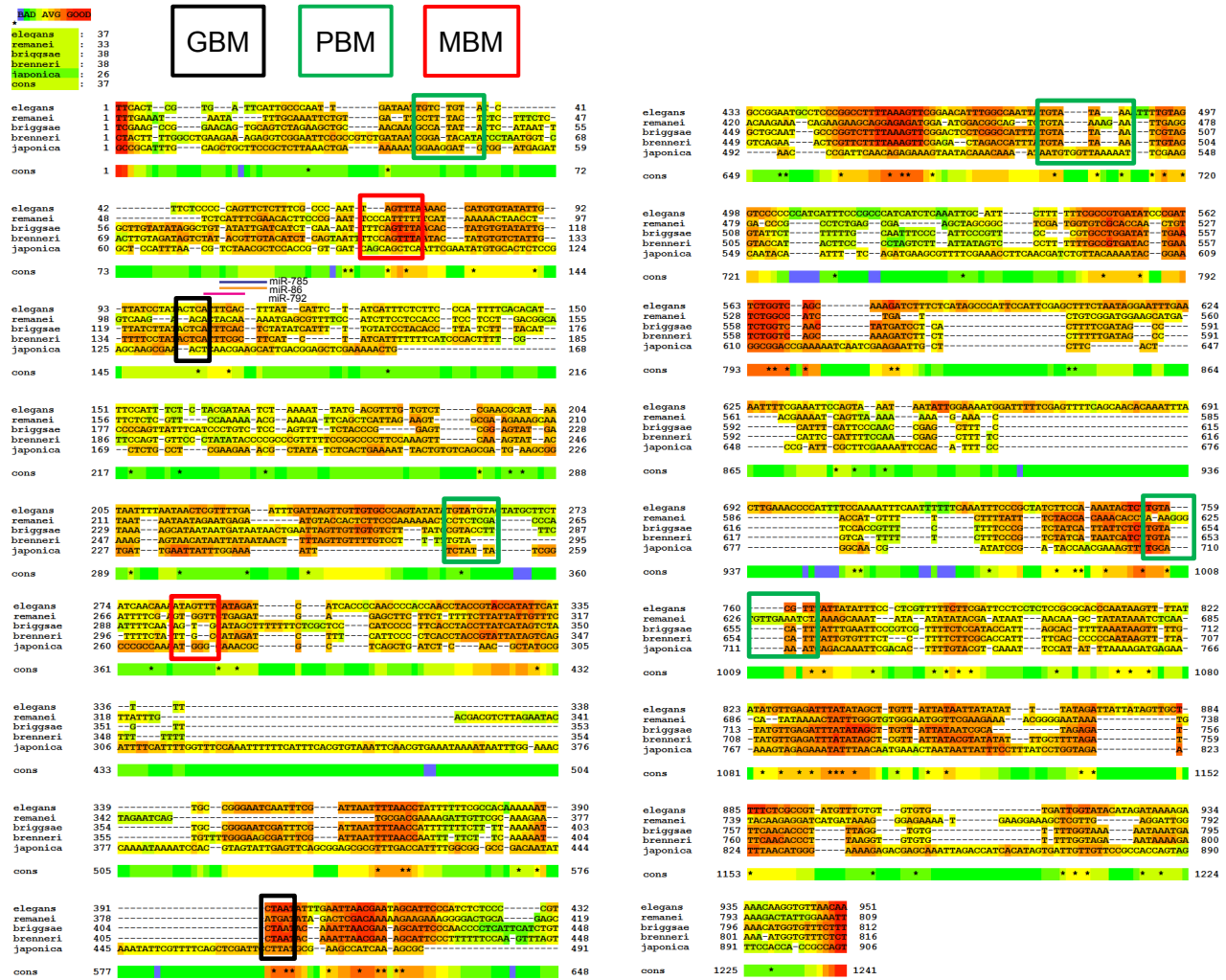
**B**



**C**



**A**



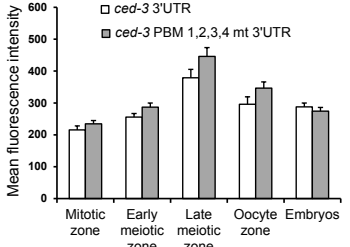
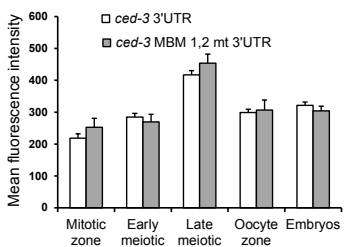
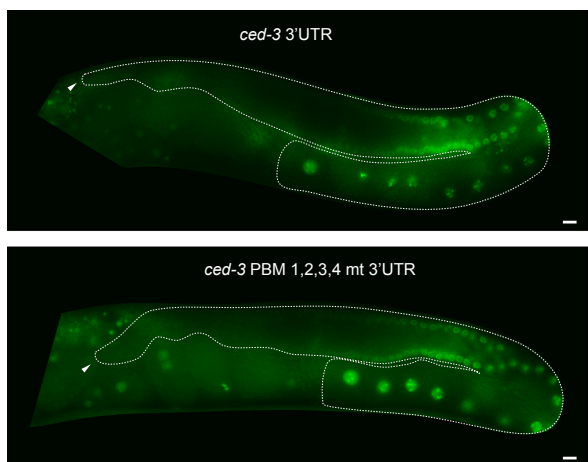
**B**

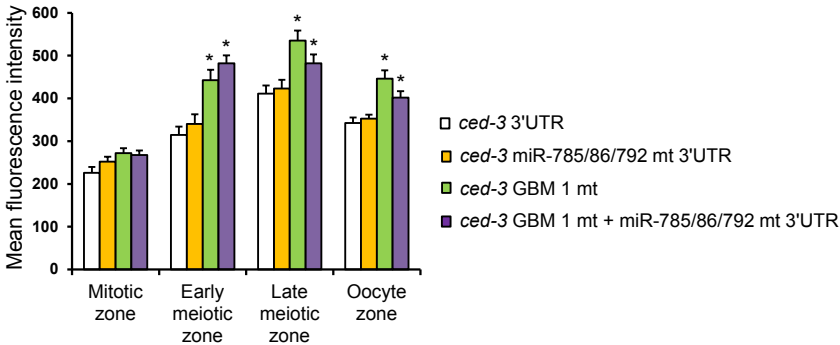
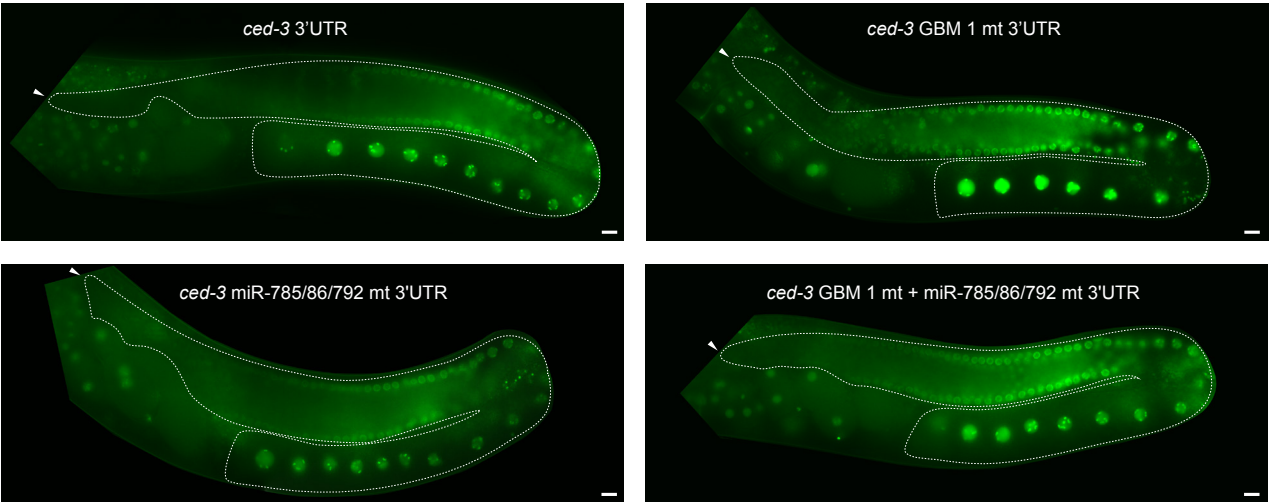
Binding motif	GLD-1 binding motif (GBM) CLIP	Predicted PUF-8 binding motif (PBM) (Opperman et al., 2005)	Predicted MEX-3 binding motif (MBM) (Pagano et al., 2009)
WT	ACUCA ↓ A	UGUAAAA ↓ CCUG	AGAGUUUA ↓ GU ↓ A
mt	GGG	CCC	CCC

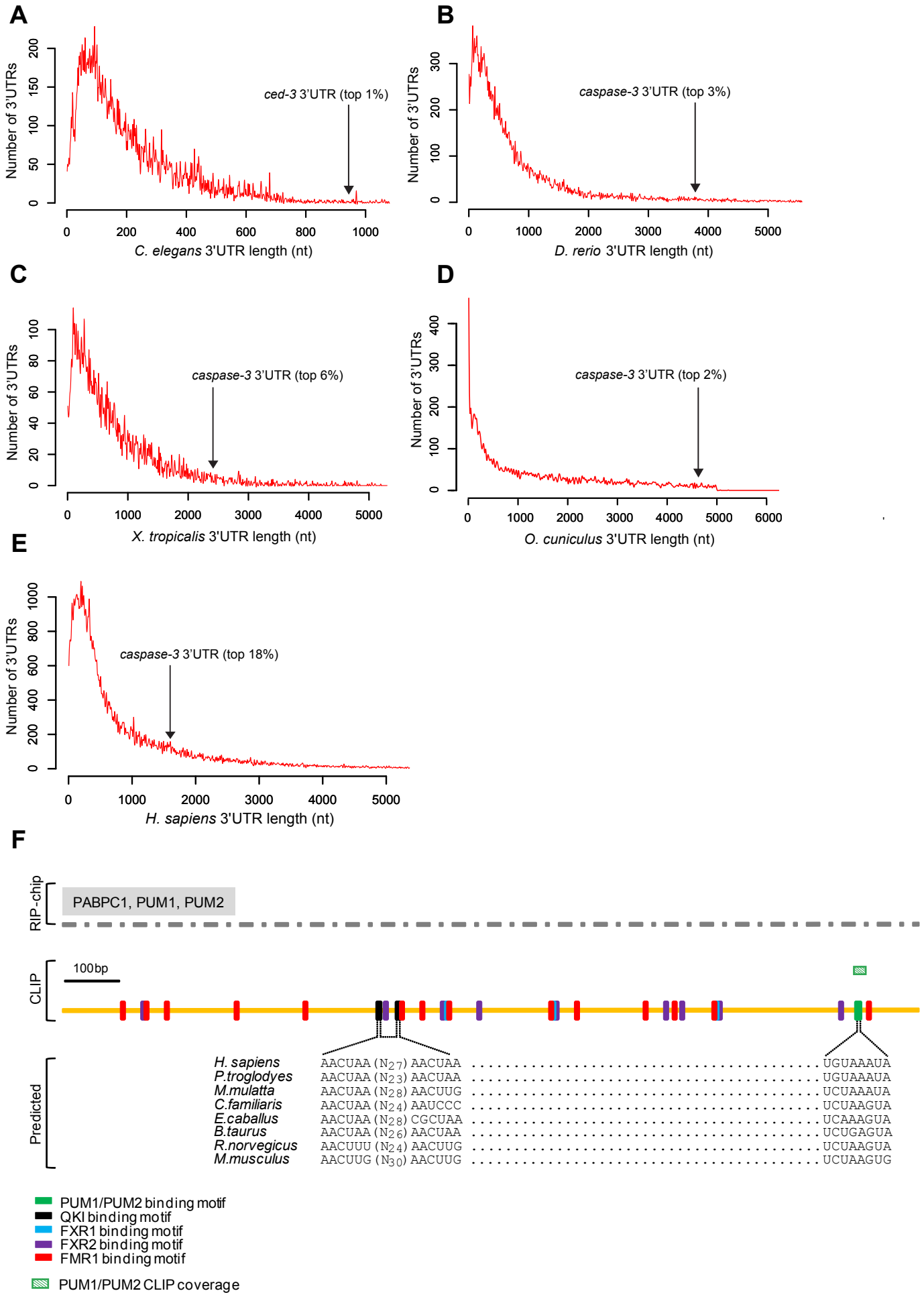
**C**



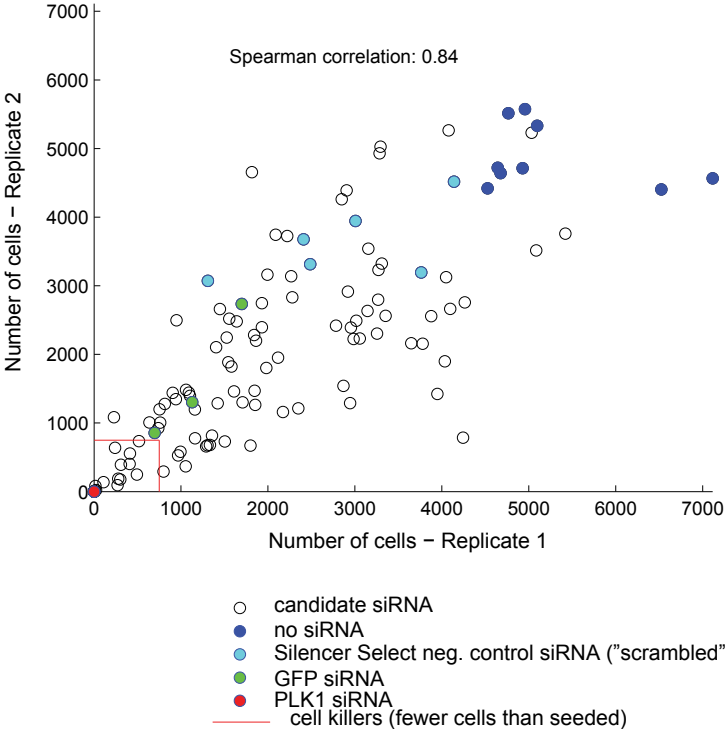
**D**





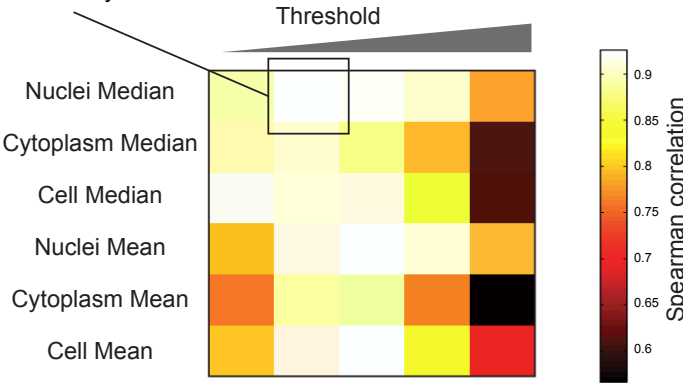


**A**



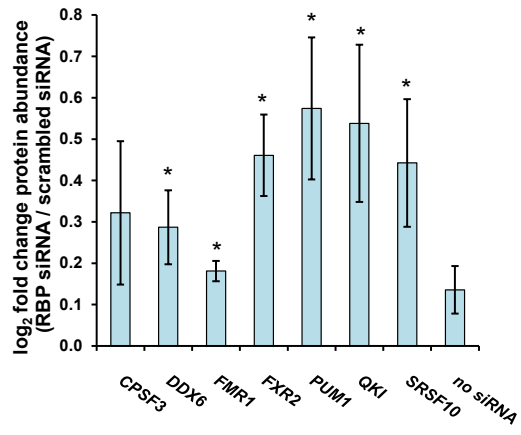
**B**

Definition for which the data were analyzed

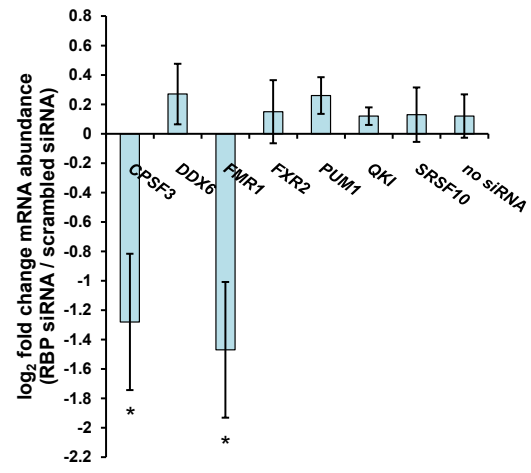




**A**



**B**



## Supplemental Tables S1 to S4

### Supplemental Table S1. RNA binding proteins used in an RNAi screen for CED-3 regulation.

Gene	Description	Changes in CED-3::GFP	Zones with changed CED-3 expression
<i>gla-3</i>	TIS11-like protein with two CCCH-like zinc-finger domains, inhibits germline apoptosis	no	/
<i>cpb-3</i>	Cytoplasmic polyadenylation element binding protein family, inhibits germline apoptosis	no	/
<i>car-1</i>	Human LSM14A and LSM14B homologue putative RBP, inhibits germline apoptosis	no	/
<i>cgh-1</i>	DEAD-box Conserved germline helicase, inhibits germline apoptosis	yes	upregulation in the late meiotic and oocyte zone
<i>gld-1</i>	KH domain protein, inhibits p53 tumor suppressor cep-1 and germline apoptosis	yes	upregulation in the early and late meiotic zone
<i>puf-3</i>	Conserved PUF (Pumilio and FBF) family of RBPs, regulates early embryogenesis	no	/
<i>puf-4</i>	Conserved PUF (Pumilio and FBF) family of RBPs	no	/
<i>puf-5</i>	Conserved PUF (Pumilio and FBF) family of RBPs, regulates oocyte maturation	no	/
<i>puf-6</i>	Conserved PUF (Pumilio and FBF) family of RBPs	no	/
<i>puf-7</i>	Conserved PUF (Pumilio and FBF) family of RBPs	no	/
<i>puf-8</i>	Conserved PUF (Pumilio and FBF) family of RBPs, maintenance of stem cell proliferation	yes	upregulation in the mitotic and early meiotic zone
<i>puf-9</i>	Conserved PUF (Pumilio and FBF) family of RBPs, controls locomotion and fluid balance	no	/
<i>puf-12</i>	Conserved PUF (Pumilio and FBF) family of RBPs	no	/
<i>fbf-1/fbf-2</i>	Conserved PUF (Pumilio and FBF) family of RBPs, maintenance of stem cell proliferation	no	/
<i>gld-2</i>	Cytoplasmic poly(A) polymerase (PAP), regulates the switch from mitosis to meiosis	no	/
<i>mex-3</i>	KH domain protein, regulates cell fate specification and germline totipotency	yes	upregulation in embryos
<i>nos-3</i>	Drosophila Nanos related, promotes the switch from sperm to oocyte production	no	/
<i>glh-1</i>	DEAD-box RNA helicase, required for proper germline development and fertility	no	/
<i>pgl-1</i>	RGG-box protein, required for germline development and P granules formation	no	/
<i>C41G7.3</i>	KH domain protein, involved in maintaining germline integrity (unpublished data)	no	/

Synchronized L1 animals expressing CED-3::GFP were transferred to plates with bacteria expressing dsRNA constructs targeting the respective RBPs. GFP intensity was quantified in 4 germline zones (mitotic zone, early meiotic zone, late meiotic zone, oocytes) and fertilized embryos of adult hermaphrodites.



**Supplemental Table S2. RNA binding proteins selected for an image-based RNAi screen for *caspase-3* regulation**

Homologs of PUF-8, GLD-1, CGH-1 and MEX-3 in humans and an additional group of RBPs that had predicted or experimentally detected binding sites in caspase-3 3'UTR by RBPDB, CLIPz or doRINA databases (Cook et al. 2011; Khorshid et al. 2011; Anders et al. 2012) were selected for RNAi screen for post-transcriptional regulation of human caspase-3.

Homologs of PUF-8, GLD-1, CGH-1 and MEX-3	RBPs with CLIP identified or predicted sites in caspase-3 3'UTR*
PUM2	SRSF1
PUM1	ZRANB2
QKI	PABPC1
KHDRBS1	RBM1A1
KHDRBS2	EIF4B
KHDRBS3	FUS
SF1	SRSF9
DDX6	MBNL1
EIF4A2	ACO1
DDX47	KHSRP
MEX3A	YTHDC1
MEX3B	RBMX
MEX3C	SRSF10
MEX3D	ELAVL1
	CPSF4
	CPSF3
	FXR2
	IGF2BP1
	FMR1

**Supplemental Table S3. Mutations in RBP and miRNA binding motifs in *ced-3* 3'UTR used to generate 3'UTR reporters ( $P_{pie-1}::gfp::h2b::ced-3(3'UTR)$ )**

Construct	WT sequence	ced 3'-UTR (nt position in 3'-UTR)	Mutant sequence
GLD-1 BM 1 mt	actcatt	(107-113)	ctgagga
GLD-1 BM 1,2 mt	ctc, cta	(108-110), (396-398)	ggg, ggg
PUF-8 BM 1,2,3,4 mt	ugu	(37-39), (261-263), (486-488), (761-763)	ccc
MEX-3 BM 1,2 mt	agu	(75-77), (290-292)	ccc
miRNA-785/86/792 mt	acttt	(116-120)	tgagg

## Supplemental Table S4. Primers used in this study

Construct or gene	Forward primer	Reverse primer	Use
GBM 1 mt	TGTGTATATTGTTATCTATCTGAGGATCACTTTATCAT	GATAGAATGATAAAGTGATCCTCAGATAGGATAACAATA	SDM of <i>ced-3</i> 3'UTR in pDONR p2R-P3
GBM 1 mt (for GBM 1, 2 mt)	TATTGTTATCCTATAGGGATTTCACCTTTATCAT	ATGATAAAGTGAAATCCCTATAGGATAACAATA	SDM of <i>ced-3</i> 3'UTR in pDONR p2R-P3
GBM 2 mt	TTCGCCACAAAAATGGGATATTTGAATTAACG	CGTAAATCAAATATCCCAATTTTTGGGCGAA	SDM of <i>ced-3</i> 3'UTR in pDONR p2R-P3
PBM 1 mt	TGCCCAATTGATAATCCCTGTATCTTCTCCCC	GGGAGAAGATACAGGGGATTATCAATTGGGCA	SDM of <i>ced-3</i> 3'UTR in pDONR p2R-P3
PBM 2 mt	TGTGCCCAGTATATACCCATGACTATGCTTCT	AGAAGCATAGTACATGGGTATATCTGGGCACA	SDM of <i>ced-3</i> 3'UTR in pDONR p2R-P3
PBM 3 mt	ACATTTGGCCAATTACCCATAAAATTTGTAGG	CCTACAAAATTTTATGGTAATTGGCCAATGT	SDM of <i>ced-3</i> 3'UTR in pDONR p2R-P3
PBM 4 mt	CTTCCAAAATACTCTCCACGTTTATTATATT	AAATAATAAAACGTGGGAGAGATTTTGGAAAG	SDM of <i>ced-3</i> 3'UTR in pDONR p2R-P3
MBM 1 mt	CTCTTTCGCCCAATCCCTTAAACCATGTGTA	TACACATGGTTTTAAGGAAATGGGCGAAAGAG	SDM of <i>ced-3</i> 3'UTR in pDONR p2R-P3
MBM 2 mt	TTCTATCAACAAAATCCCTCATAGATCATCAC	GTGATGATCTATGAAGGGATTTTGTGATAGAA	SDM of <i>ced-3</i> 3'UTR in pDONR p2R-P3
miRNA-785/86/792 BM mt	GTTATCCTACTACTTTCTGCGGATCATCTATCTTCTCTTC	GAAGAGAAATGATAGAATGATCCGAGAAATGAGTATAGGATAAC	SDM of <i>ced-3</i> 3'UTR in pDONR p2R-P3
<i>cep-1</i>	TAATACGACTCACTATAGGgcatgaaactgccaaag	TACGAACAACTTTATTCG	Biotinylated RNA synthesis from plasmids generated via SDM
<i>ced-3</i>	TAATACGACTCACTATAGGtaaaattcactcgtgattcattgcc	GTATACCAATCACACACACAAAC	Biotinylated RNA synthesis from genomic DNA
<i>RASM</i>	TAATACGACTCACTATAGGgacatacaagctggtggg	CACATTGCAGTTTGTGGG	Biotinylated RNA synthesis from HEK cells
<i>pgk-1</i>	GCGATATTTATGTCATGATGCTTTC	TGAGTGCTCGACTCCAACCA	qRT-PCR, normalization controls
<i>cdc-42</i>	CTGCTGGACAGGAAGATTACG	CTCGGACATTCTGCAATGAAG	qRT-PCR, normalization-controls
<i>Y45F10D.4</i>	GTCGCTCAAATCAGTTACG	GTTCTTGCAAAGTATCCGACA	qRT-PCR, normalization controls
<i>ced-3</i>	CATTTCATCGGATCGACACAA	TGAAGAGTTGGCGGATGAA	qRT-PCR
<i>cep-1</i>	TTTTTTGGACGATGAAAATGGA	AATCCITTTGTTTTGGCTTTC	qRT-PCR
<i>rme-2</i>	AGTGAGCAACGTGGCAGTC	AGCGCTTGGAGATGGAGAT	qRT-PCR
<i>tra-2</i>	CATCGAATCGCAGTTGTCTG	TCGCCTTGATAGTTGGTGTG	qRT-PCR
<i>puf-5</i>	GGATCCTTCGATGGAGGTG	TTCCAGTTCCTCATGAAGTT	qRT-PCR
<i>pie-1</i>	GATGAGCTGAGAGTTCCGAGA	TGTATCCACGTCGTCTCGTC	qRT-PCR
<i>mpk-1</i>	TGCTCAGTAATCGGCCATTG	TCCAACAACCTGCCAAAATCAAA	qRT-PCR
<i>rgef-1</i>	GGCTTCGAGCAGTTTCAGTT	TAGGGGATGCTTGGACAAA	qRT-PCR
<i>pah-1</i>	CATCGCCATTCATAACATCAG	TCACGACGATCCTTGGAC	qRT-PCR
<i>pos-1</i>	CTACGGCTCAATGGCACA	GGGAGGAGAGCTGCTGAAT	qRT-PCR
<i>nos-2</i>	AAATGAATCACACCGGAGACGTA	GGAATGCTTGTAATAATGATAACG	qRT-PCR
<i>spn-4</i>	AGAGCGACAGCTTTCAGACG	GAAACGATGGGAACTTCG	qRT-PCR

## References

- Anders G, Mackowiak SD, Jens M, Maaskola J, Kuntzagk A, Rajewsky N, Landthaler M, Dieterich C. 2012. doRiNA: a database of RNA interactions in post-transcriptional regulation. *Nucleic acids research* **40**: D180-6.
- Ascano M, Mukherjee N, Bandaru P, Miller JB, Nusbaum JD, Corcoran DL, Langlois C, Munschauer M, Dewell S, Hafner M et al. 2012. FMRP targets distinct mRNA sequence elements to regulate protein expression. *Nature* **492**: 382–386.
- Brümmer A, Kishore S, Subasic D, Hengartner M, Zavolan M. 2013. Modeling the binding specificity of the RNA-binding protein GLD-1 suggests a function of coding region-located sites in translational repression. *RNA* **19**: 1317–1326.
- Cook KB, Kazan H, Zuberi K, Morris Q, Hughes TR. 2011. RBPDB: a database of RNA-binding specificities. *Nucleic acids research* **39**: D301-8.
- Dassi E, Re A, Leo S, Tebaldi T, Pasini L, Peroni D, Quattrone A. 2014. AURA 2: Empowering discovery of post-transcriptional networks. *Translation (Austin, Tex.)* **2**: e27738.
- Galarneau A, Richard S. 2005. Target RNA motif and target mRNAs of the Quaking STAR protein. *Nature structural & molecular biology* **12**: 691–698.
- Galgano A, Forrer M, Jaskiewicz L, Kanitz A, Zavolan M, Gerber AP. 2008. Comparative analysis of mRNA targets for human PUF-family proteins suggests extensive interaction with the miRNA regulatory system. *PloS one* **3**: e3164.
- Hafner M, Landthaler M, Burger L, Khorshid M, Hausser J, Berninger P, Rothballer A, Ascano M, Jungkamp A, Munschauer M et al. 2010. Transcriptome-wide Identification of RNA-Binding Protein and MicroRNA Target Sites by PAR-CLIP. *Cell* **141**: 129–141.
- Jungkamp A, Stoeckius M, Mecnas D, Grün D, Mastrobuoni G, Kempa S, Rajewsky N. 2011. In vivo and transcriptome-wide identification of RNA binding protein target sites. *Mol. Cell* **44**: 828–840.
- Kent WJ. 2002. BLAT--the BLAST-like alignment tool. *Genome research* **12**: 656–664.
- Kent WJ, Sugnet CW, Furey TS, Roskin KM, Pringle TH, Zahler AM, Haussler D. 2002. The human genome browser at UCSC. *Genome research* **12**: 996–1006.
- Khorshid M, Rodak C, Zavolan M. 2011. CLIPZ: a database and analysis environment for experimentally determined binding sites of RNA-binding proteins. *Nucleic acids research* **39**: D245-52.
- Morris AR, Mukherjee N, Keene JD. 2008. Ribonomic analysis of human Pum1 reveals cis-trans conservation across species despite evolution of diverse mRNA target sets. *Molecular and cellular biology* **28**: 4093–4103.
- Mukherjee N, Lager PJ, Friedersdorf MB, Thompson MA, Keene JD. 2009. Coordinated posttranscriptional mRNA population dynamics during T-cell activation. *Molecular systems biology* **5**: 288.
- Opperman L, Hook B, DeFino M, Bernstein DS, Wickens M. 2005. A single spacer nucleotide determines the specificities of two mRNA regulatory proteins. *Nat. Struct. Mol. Biol.* **12**: 945–951.
- Pagano JM, Farley BM, Essien KI, Ryder SP. 2009. RNA recognition by the embryonic cell fate determinant and germline totipotency factor MEX-3. *Proc. Natl. Acad. Sci. U.S.A.* **106**: 20252–20257.
- Schumacher B, Hanazawa M, Lee M, Nayak S, Volkmann K, Hofmann ER, Hofmann R, Hengartner M, Schedl T, Gartner A. 2005. Translational repression of *C. elegans* p53 by GLD-1 regulates DNA damage-induced apoptosis. *Cell* **120**: 357–368.
- Wang X, McLachlan J, Zamore PD, Hall TMT. 2002. Modular recognition of RNA by a human pumilio-homology domain. *Cell* **110**: 501–512.